Turning lignin into a recyclable bioresource: transesterification vitrimers from lignins modified with ethylene carbonate

Antoine Duval,[1,2,*] Wissem Benali,[1] Luc Avérous[1,*]

[1] BioTeam/ICPEES-ECPM, UMR CNRS 7515, Université de Strasbourg, 25 rue Becquerel, 67087 Strasbourg Cedex 2, France

[2] Soprema, 15 rue de Saint Nazaire, 67100 Strasbourg, France

* Corresponding authors: antoine.duval@unistra.fr, luc.averous@unistra.fr

SUPPLEMENTARY INFORMATION

24 Figures, 12 Tables

Characterization of PEG-COOH

PEG-COOH was characterized by ^{1}H (Figure S 1) and ^{31}P NMR (Figure S 2). Both were used to calculate the content in COOH groups.
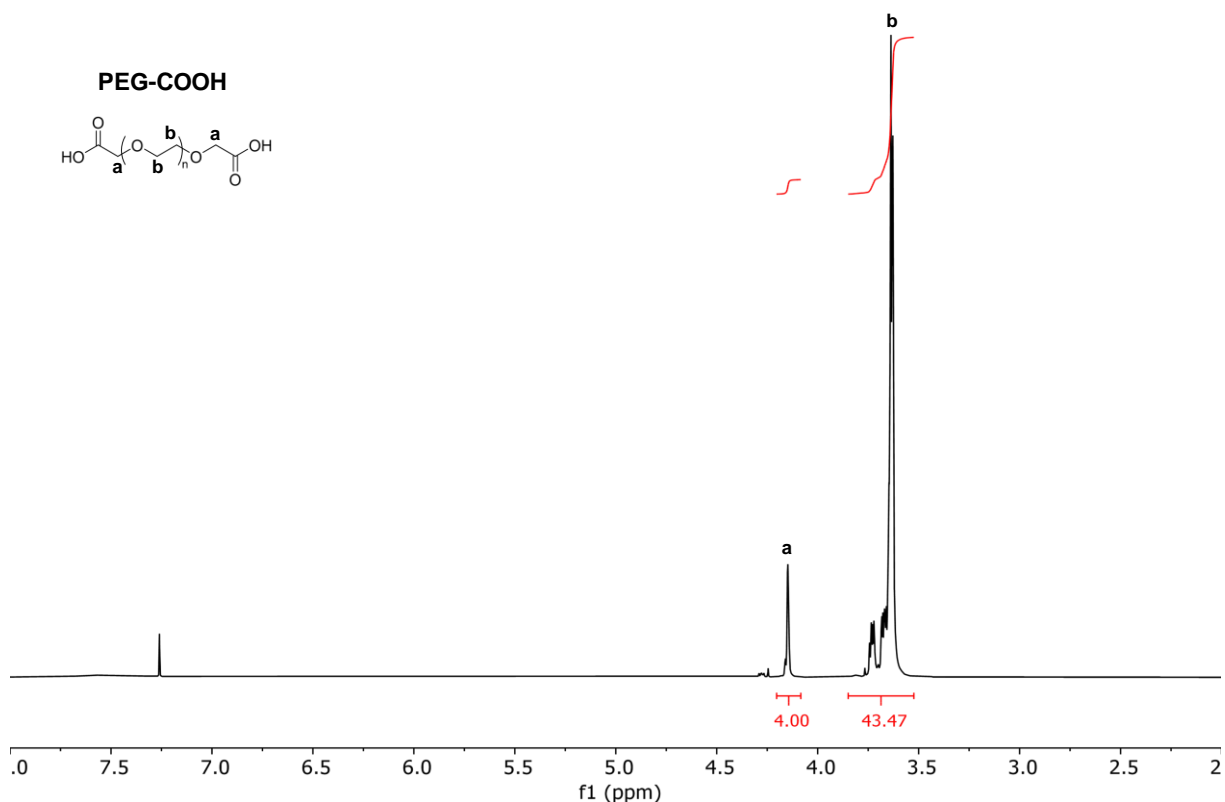

Figure S 1. ^{1}H NMR (CDCl$_3$, 400 MHz) of PEG-COOH

From ^{1}H NMR data, the average degree of polymerization (n) of the PEG motif was calculated as:

$$n = \frac{\int b}{m} = \frac{43.47}{4} = 10.9$$

with **b** the signal of the proton in PEG repeat unit -CH$_2$-CH$_2$-O- (Figure S 1), and *m* the corresponding multiplicity (4H).

The average molar mass M_n is then calculated as:

$$M_n \ (g \ mol^{-1}) = 44 \times n + 134 = 612$$

with 44 g mol^{-1} the average molar mass of the PEG repeat unit (-CH$_2$-CH$_2$-O-) and 134 g mol^{-1} the molar mass of the chain ends.

The obtained M_n is in good agreement with supplier data (600 g mol^{-1}). The average content in COOH functions is then calculated as **3.27 mmol g^{-1}**.
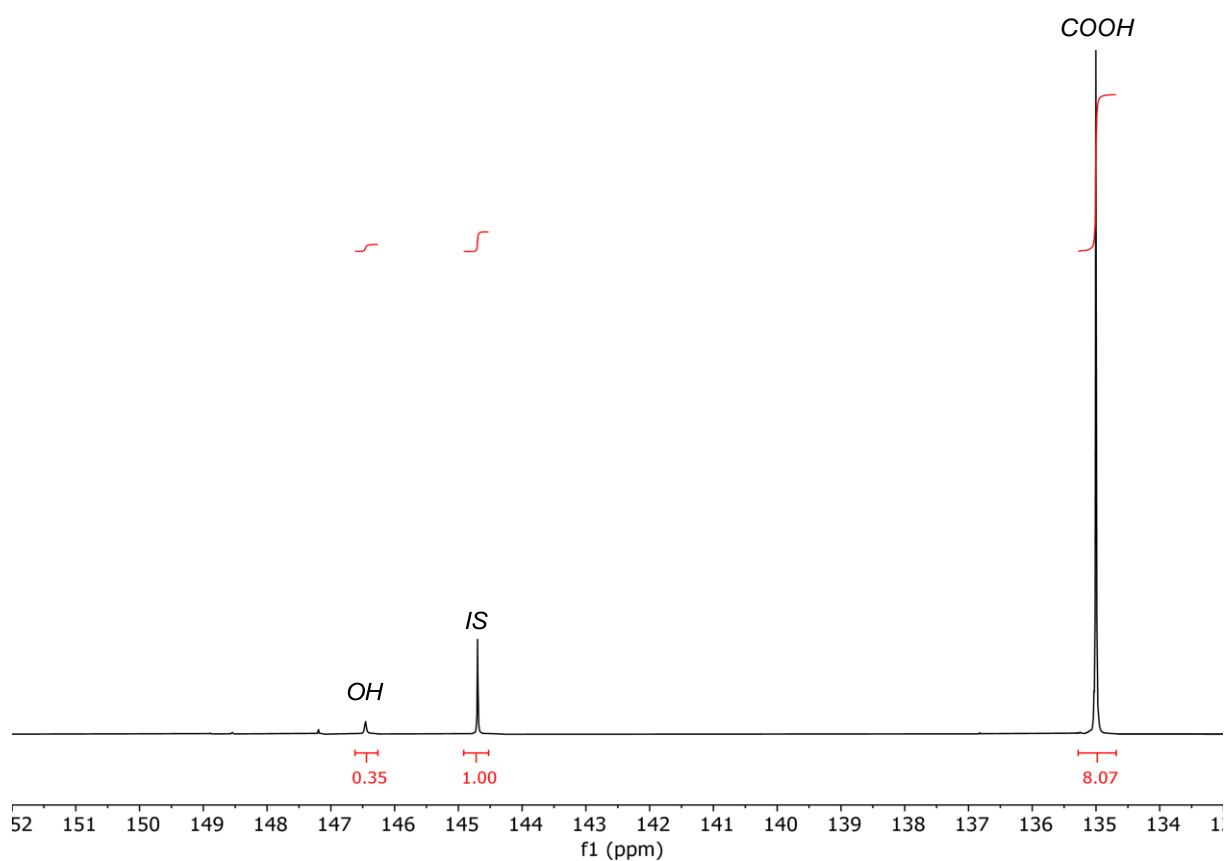
Figure S 2. ^{31}P NMR of PEG-COOH. IS = internal standard (cholesterol).

^{31}P NMR (Figure S 2) data show that PEG-COOH has mostly COOH chain ends. Only negligible amounts of residual OH chain ends are detected (4.1%). The COOH content is calculated as **3.52 mmol g^{-1}**, in fair agreement with the ^1H NMR results.

Chemical modification of KL with EC

Table S 1. Reaction conditions used for the modification of KL with EC

#	m_{KL} (g)	EC (eq)	T (°C)	t (h)	Conversion by ^{31}P NMR (%)	
					Ph-OH	*COOH*
1	5	3	110	1	*ins*	*ins*
2	5		110	1	53.3	83.2
3	5	5	110	1	54.5	97.2
4	1		110	2	36.0	75.1
5	1		120	1	*ins*	*ins*
6	1		110	1	47.9	76.1
7	1		110	3	95.0	96.3
8	5		110	3	*ins*	*ins*
9	5	7	120	1	*ins*	*ins*
10	32.5		110	1	*ins*	*ins*
11	32.5		100	2	75.4	100.0
12	32.5		100	3	100.0	100.0
13	32.5		100	3	100.0	100.0

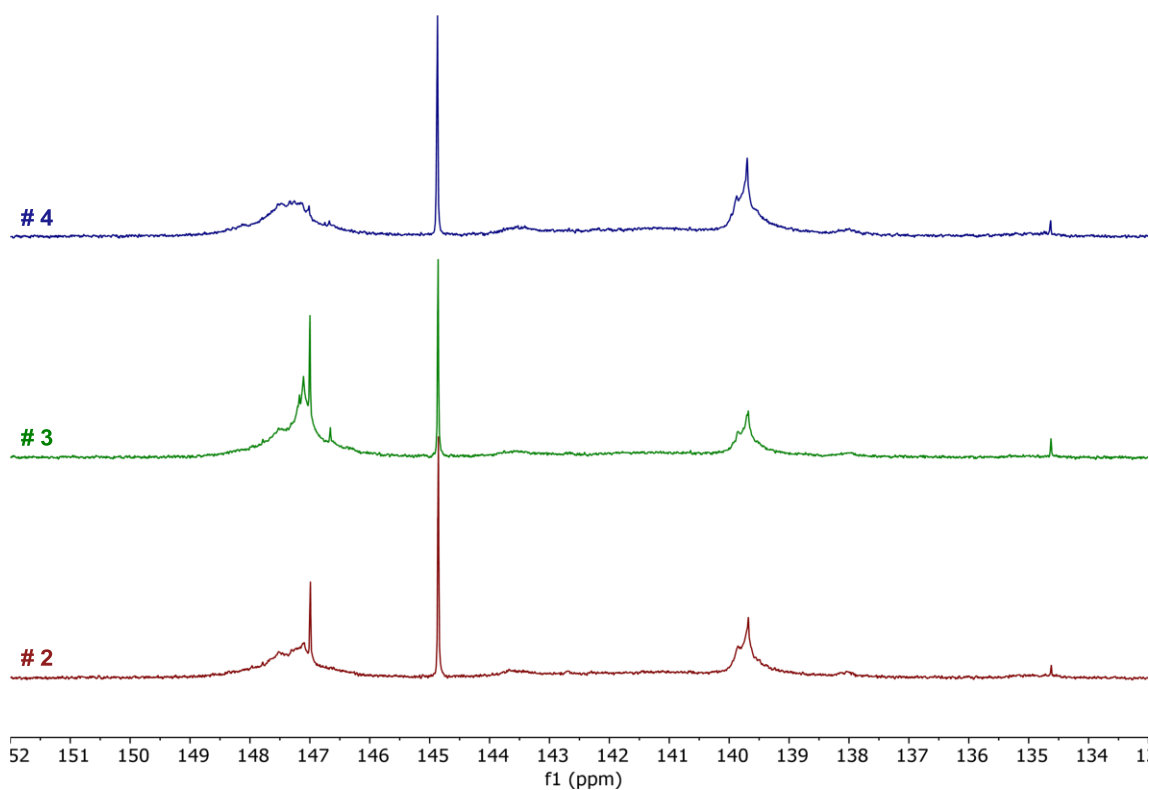*ins* = insoluble product, not analyzed by ^{31}P NMR

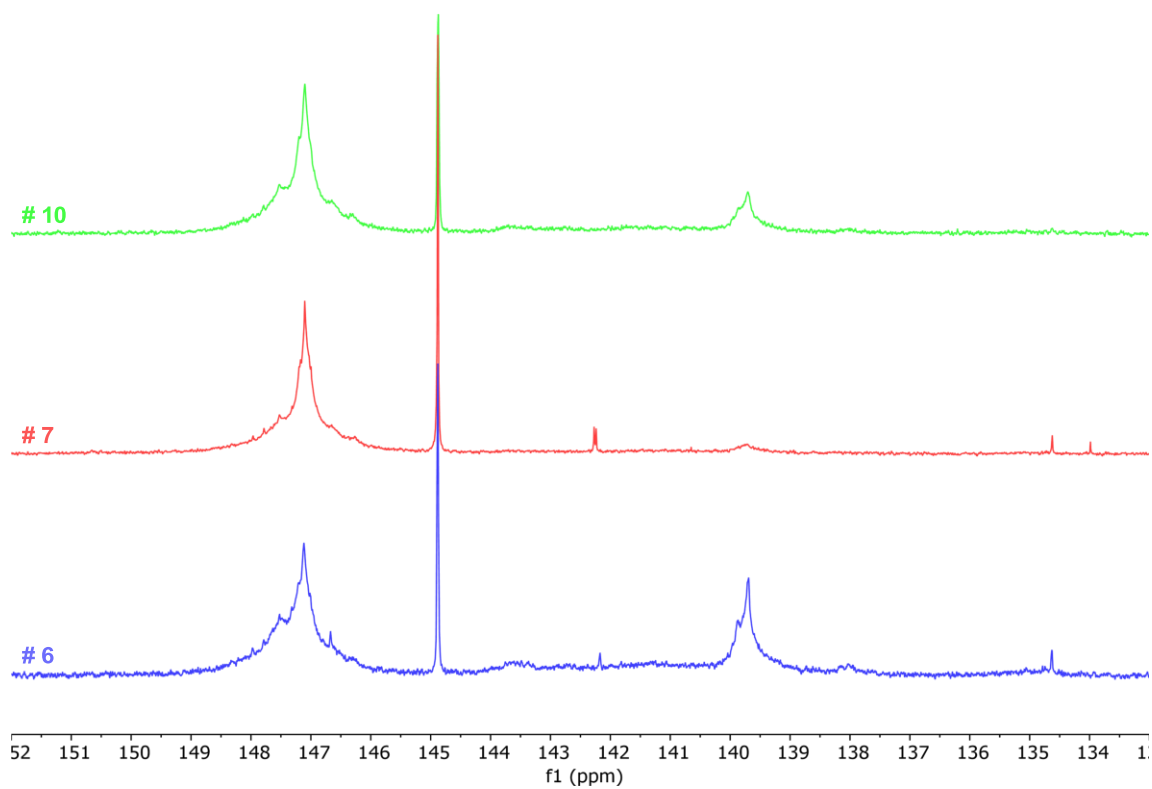*Figure S 3. ^{31}P NMR spectra of KL after reaction with 5 equivalents EC. Conditions described in Table S1.*

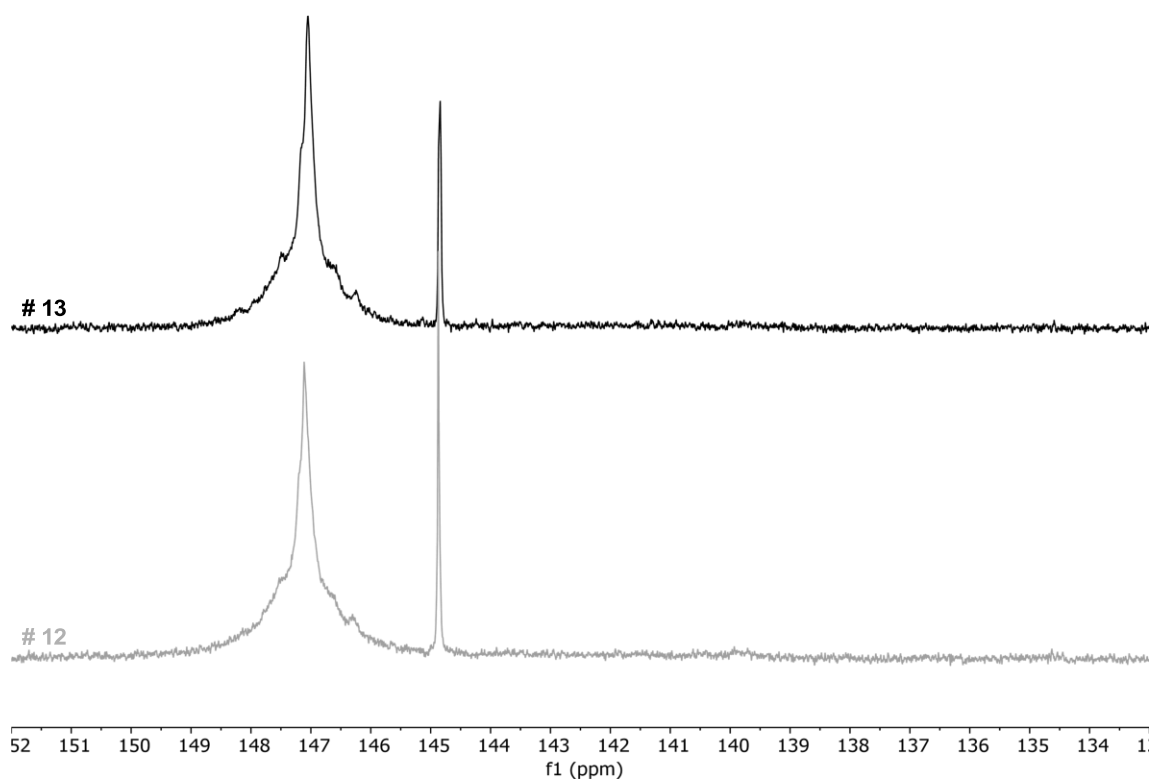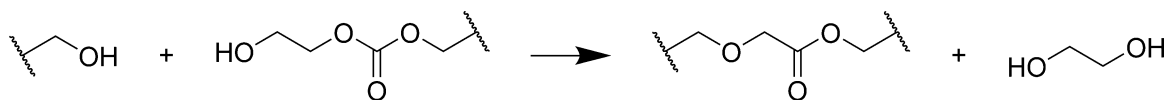*Figure S 4. ^{31}P NMR spectra of KL after reaction with 7 equivalents EC. Conditions described in Table S1.*

Figure S 5. ^{31}P NMR spectra of KL after reaction with 7 equivalents EC, under optimized conditions. Conditions described in Table S1.

Scheme S 1. Possible crosslinking side reaction during the modification of KL with EC.

Figure S 6. Aromatic regions of the HSQC NMR spectra of (a) KL and (b) KL.EC.

Predicted shifts
β   1.75 / 34.2 ppm
β'   1.85 / 30.8 ppm
β''   2.00 / 29.7 ppm

Experimental shifts
β   1.72 / 35.1 ppm
β'   1.91 / 30.5 ppm

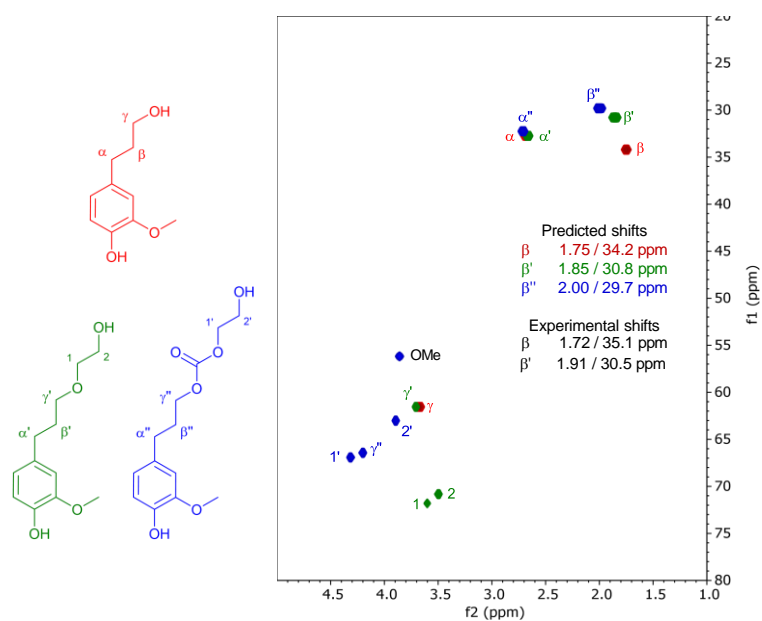*Figure S 7. Overlay of predicted HQSC NMR spectra of lignin aryl propanol end groups, etherified or carbonated at the primary OH.*

Predicted shifts
α   4.83 / 72.8 ppm
α' 4.77 / 81.6 ppm
α" 6.01 / 77.3 ppm

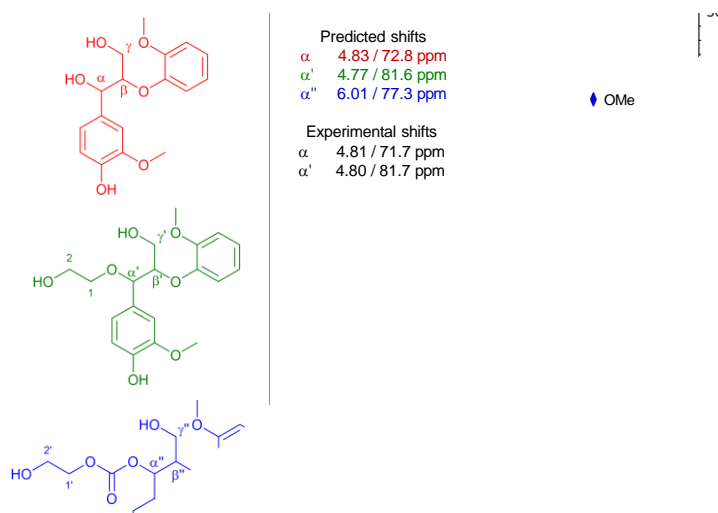Experimental shifts
α   4.81 / 71.7 ppm
α' 4.80 / 81.7 ppm

♦ OMe

Figure S 8. Overlay of predicted HQSC NMR spectra of lignin β-O-4 structure, etherified or carbonated at the secondary OH.
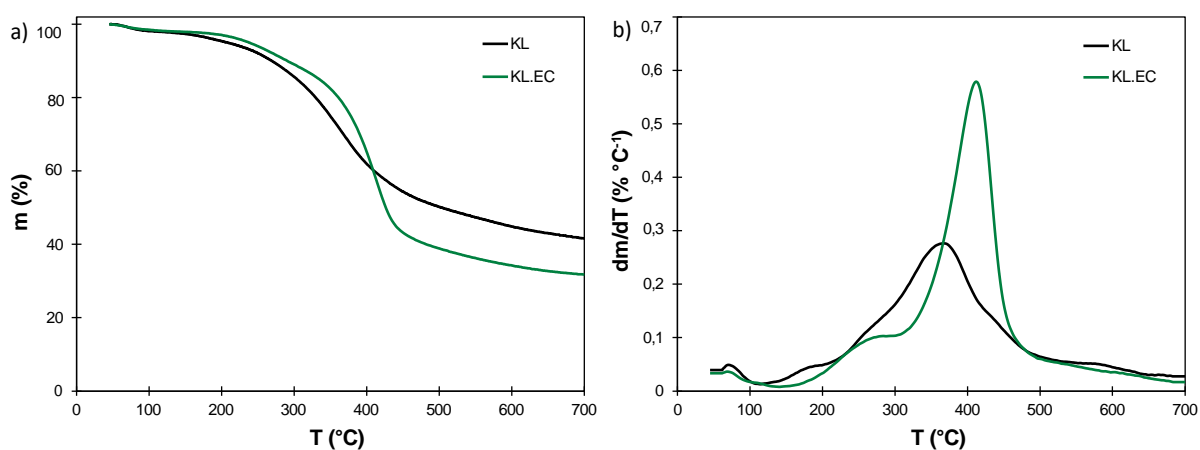

Figure S 9. TGA of KL and KL.EC: (a) mass loss and (b) derivative weight loss (DTG curves).
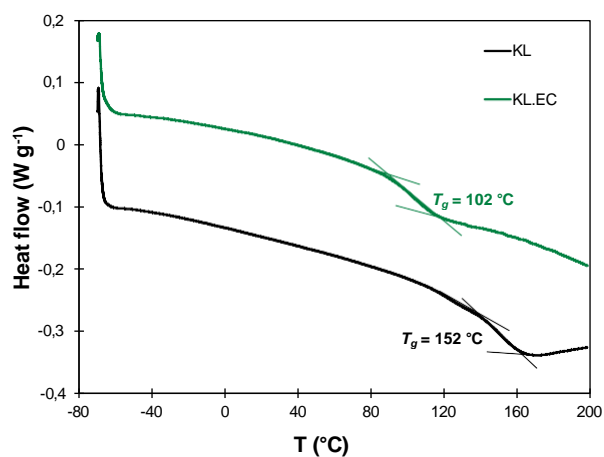
Figure S 10. DSC thermograms of KL and KL.EC.

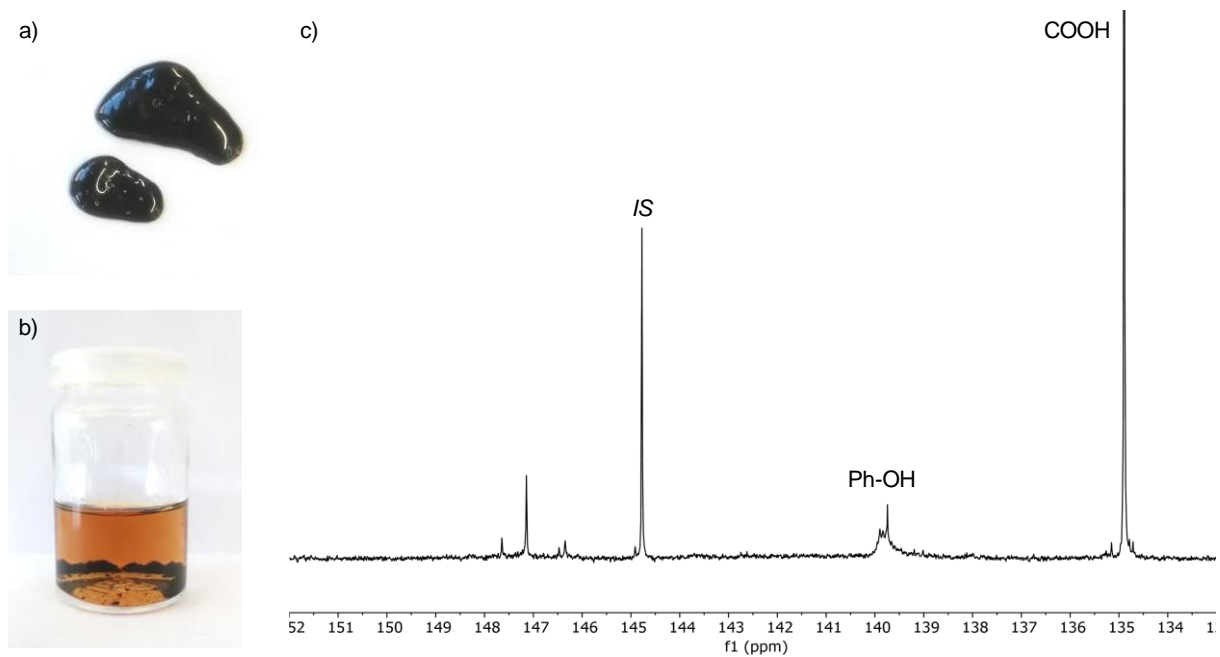*Characterization of L-PES*

a)

b)

c)

Figure S 11. Pictures of control material synthesized from neat KL and PEG-COOH: (a) after curing step and (b) after immersion in acetone/water. (c) ^{31}P NMR of the soluble fraction shows the presence of COOH and Ph-OH groups, indicating incomplete esterification.
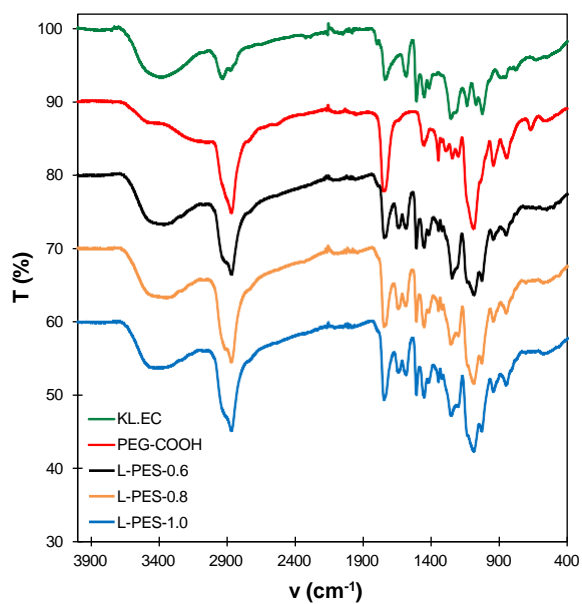

Figure S 12. FTIR spectra of KL.EC, PEG-COOH and materials L-PES-0.6, 0.8 and 1.0

Calculation of energy efficiency of materials synthesis

The energy efficiency of the materials synthesis was evaluated by calculating the metric (P6-GCM) developed by Kreuder et al.[1] It takes into account the pressure and temperature of the different steps, according to equation S1:

$$P6 - GCM = \frac{\sum(SF_P + SF_T) \times t \times m_{raw\ materials}}{m_{product}}$$

where SF_P and SF_T stand for severity factors for pressure and temperature, respectively.

SF_P and SF_T are calculated from Table S 2 and Table S 3, respectively. Eventual differences between the mass of the raw materials and final product were neglected.

Table S 2. Severity factor related to pressure[1]

Pressure range	SF_P
High pressure (> 1 atm)	7
Ambient (1 atm)	1
Vacuum (0 atm)	3

Table S 3. Severity factor related to temperature[1]

Temperature range	SF_T
Below 0 °C	7
0 °C	5
0 – 20 °C	3
Room temperature (20 – 30 °C)	1
30 – 100 °C	3
100 °C	5
> 100 °C	7

The calculation for the developed process is given in Table S 4. The most impactful step is the drying of the lignin after the modification with EC. Despite this additional step, the energy efficiency is far better than those of the direct polycondensation of neat lignin with PEG and citric acid, [2] which requires long curing time at high temperature (Table S 5).

Table S 4. Calculation of P6-GCM for the developed lignin-based polyesters synthesis

Processing step	Pressure / SF_P	Temperature / SF_T	t (h)	P6-GCM
Step 1 (EC modification)	Ambient / 1	100 ° C / 5	3	
Step 2 (drying)	Vacuum / 3	40 °C / 3	16	
Step 3 (polyester synthesis)	Vacuum / 3	120 °C / 7	1	197.5
Step 4 (hot press)	Ambient / 1	160 °C / 7	0.5	
Step 5 (post cure)	Ambient / 1	160 °C / 7	2	

Table S 5. Calculation of P6-GCM for lignin-based polyesters synthesis according to Xu et al.[2]

Processing step	Pressure / SF_P	Temperature / SF_T	t (h)	P6-GCM
Step 1 (solvent evaporation)	Ambient / 1	Ambient / 1	24	
Step 2 (curing)	Ambient / 1	110 °C / 7	48	576
Step 3 (washing / drying)	Vacuum / 3	Ambient / 1	72	

The energy efficiency of other processes for the synthesis of lignin-based polyester vitrimers was also calculated for comparison. When lignin is modified to expose carboxylic acid groups (by ozonation or modification with an anhydride) and reacted with an epoxy,[3,4] or modified with epichlorhydrin and reacted with a polycarboxylic acid,[5] the curing times are similar to our study. The main difference then comes from the modification step, and especially from eventual drying steps under vacuum.

Table S 6. Calculation of P6-GCM for lignin-based polyesters synthesis according to Zhang et al.[3]

Processing step	Pressure / SF_P	Temperature / SF_T	t (h)	P6-GCM
Step 1 (ozonation)	Ambient / 1	Ambient / 1	1	
Step 2 (drying)	Vacuum / 3	50 °C / 3	48	
Step 3 (solvent evaporation)	Vacuum / 3	50 °C / 3	na [1]	454
Step 4 (hot press)	Ambient / 1	150 °C / 7	1	
	Ambient / 1	190 °C / 7	2	

[1] This step was omitted in the calculation since the time was not available

Table S 7. Calculation of P6-GCM for lignin-based polyesters synthesis according to Hao et al.[4]

Processing step	Pressure / SF_P	Temperature / SF_T	t (h)	P6-GCM
Step 1 (reaction with anhydride)	Ambient / 1	60 °C / 3	12	
Step 2 (drying)	Vacuum / 3	50 °C / 3	12	
Step 3 (solvent evaporation)	Ambient / 1	Ambient / 1	1	169
	Ambient / 1	80 °C / 3	1	
Step 4 (curing)	Ambient / 1	150 °C / 7	1	
Step 5 (post cure)	Ambient / 1	190 °C / 7	2	

Table S 8. Calculation of P6-GCM for lignin-based polyesters synthesis according to Du et al.[5]

Processing step	Pressure / SF_P	Temperature / SF_T	t (h)	P6-GCM
Step 1 (reaction with epichlorhydrin)	Ambient / 1	Ambient / 1	120	
Step 2 (drying)	Vacuum / 3	50 °C / 3	24	
Step 3 (material synthesis)	Ambient / 1	120 °C / 7	3	469
	Ambient / 1	150 °C / 7	4	
	Ambient / 1	190 °C / 7	12	

Figure S 13. TGA of the materials: (a) mass loss and (b) derivative weight loss (DTG curves).
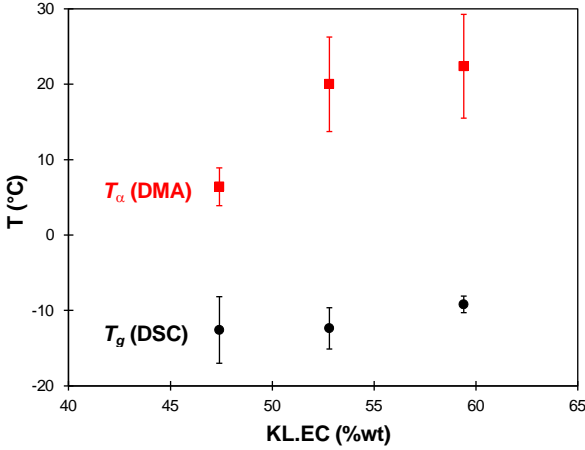

Figure S 14. Evolution of T_g and T_α with the content in KL.EC of the L-PES materials.
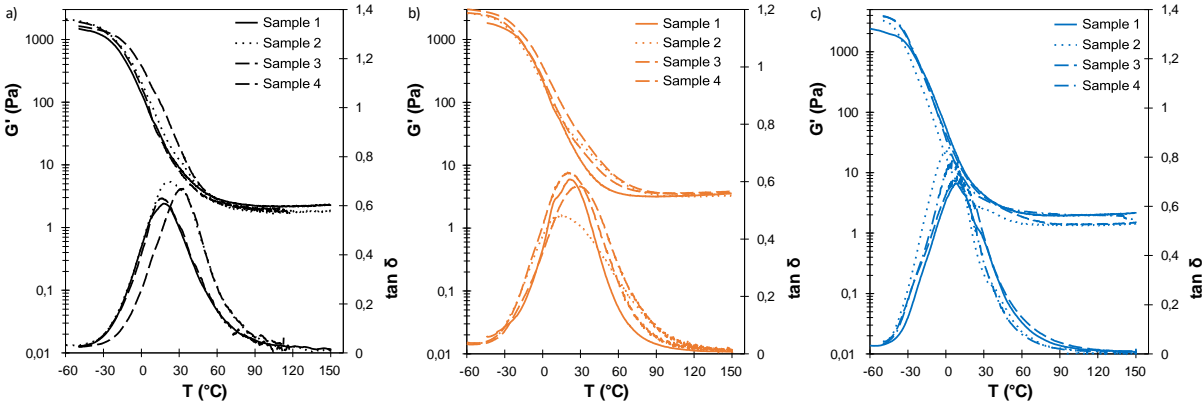

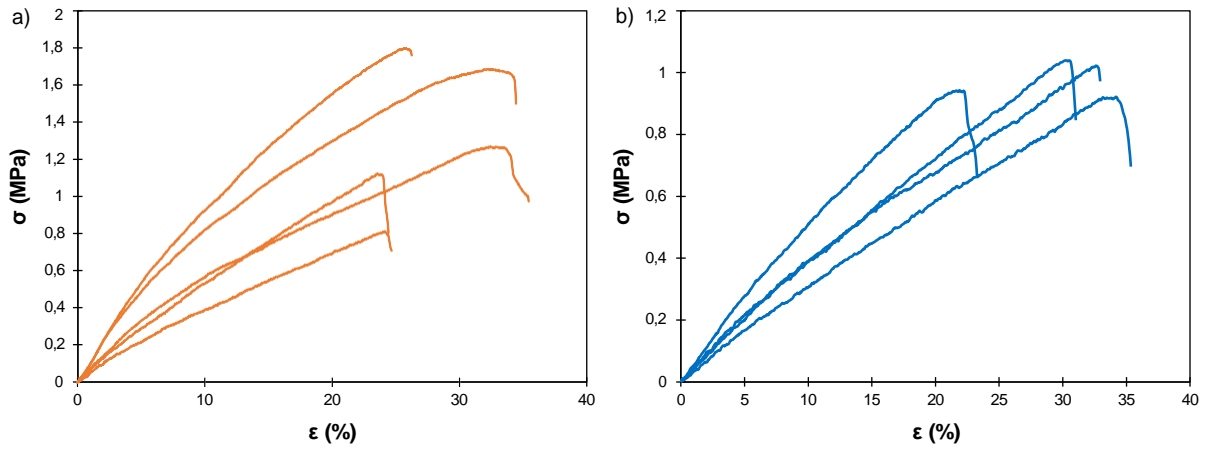*Figure S 15. Replicates of DMA of (a) L-PES-0.6, (b) L-PES-0.8 and (c) L-PES.1.0.*

Figure S 16. Stress-strain curves of (a) L-PES-0.8 and (b) L-PES-1.0.

Stress relaxation

Table S 9. Results of the fits of normalized stress relaxation data of L-PES.0.6

T (°C)	τ^* (s)	β	$\langle\tau\rangle$ (s)	G_{perm} / G_0	R^2
220	119	0.69	152	0.15	> 0.999
230	79	0.62	114	0.15	> 0.999
240	53	0.55	91	0.15	> 0.999
250	33	0.50	66	0.15	> 0.999

Table S 10. Results of the fits of normalized stress relaxation data of L-PES.0.8

T (°C)	τ^* (s)	β	$\langle\tau\rangle$ (s)	G_{perm} / G_0	R^2
220	229	0.72	285	0.22	> 0.999
230	144	0.64	200	0.22	> 0.999
240	103	0.61	153	0.22	> 0.999
250	74	0.60	112	0.22	> 0.999

Table S 11. Results of the fits of normalized stress relaxation data of L-PES.1.0

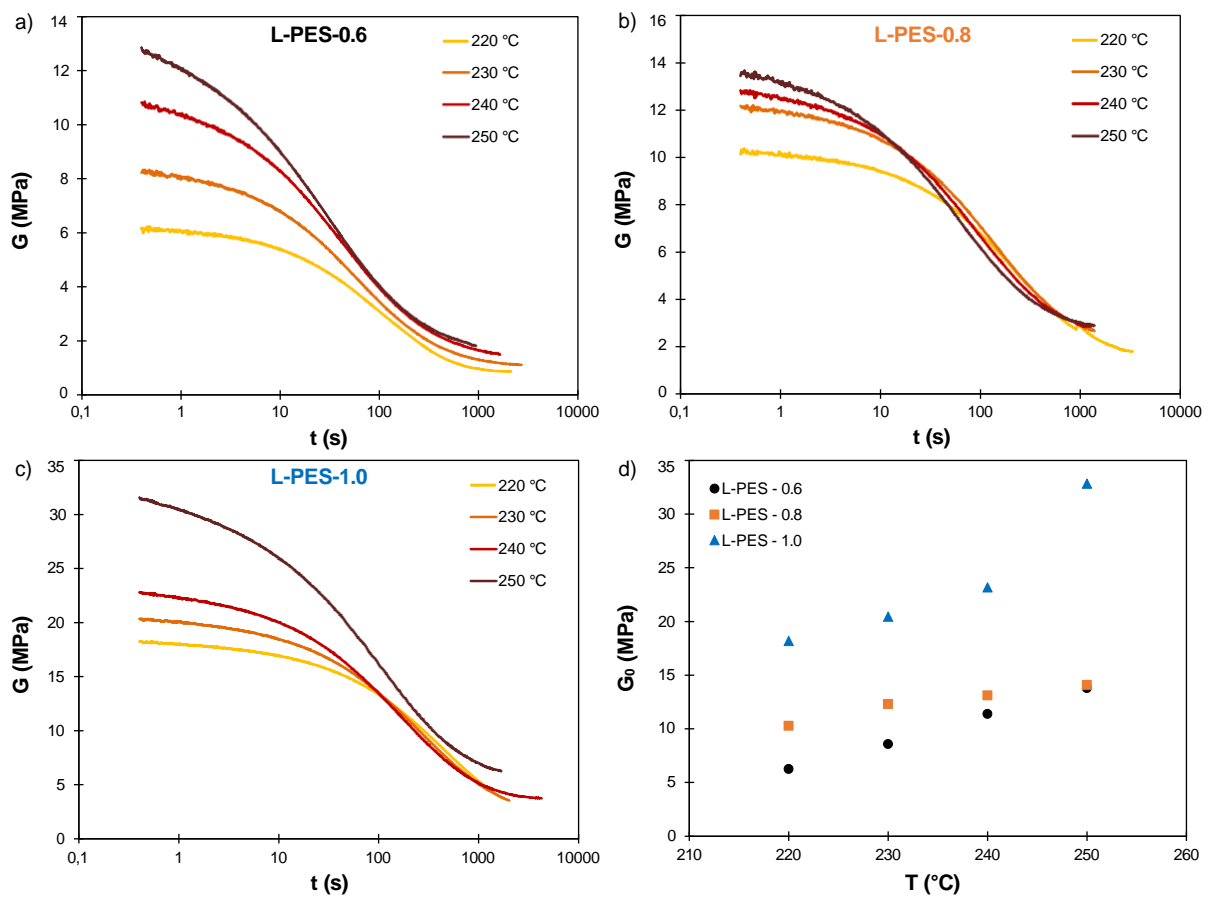| T (°C)	τ^* (s)	β	$\langle\tau\rangle$ (s)	G_{perm} / G_0	R^2
220	407	0.65	558	0.15	0.999
230	278	0.61	407	0.15	> 0.999
240	191	0.57	311	0.15	> 0.999
250	119	0.48	258	0.15	0.999

Figure S 17. Non-normalized stress relaxation curves of (a) L-PES-0.6, (b) L-PES.0.8 and (c) L-PES.1.0. (d) Evolution of the initial modulus G_0 with the temperature.
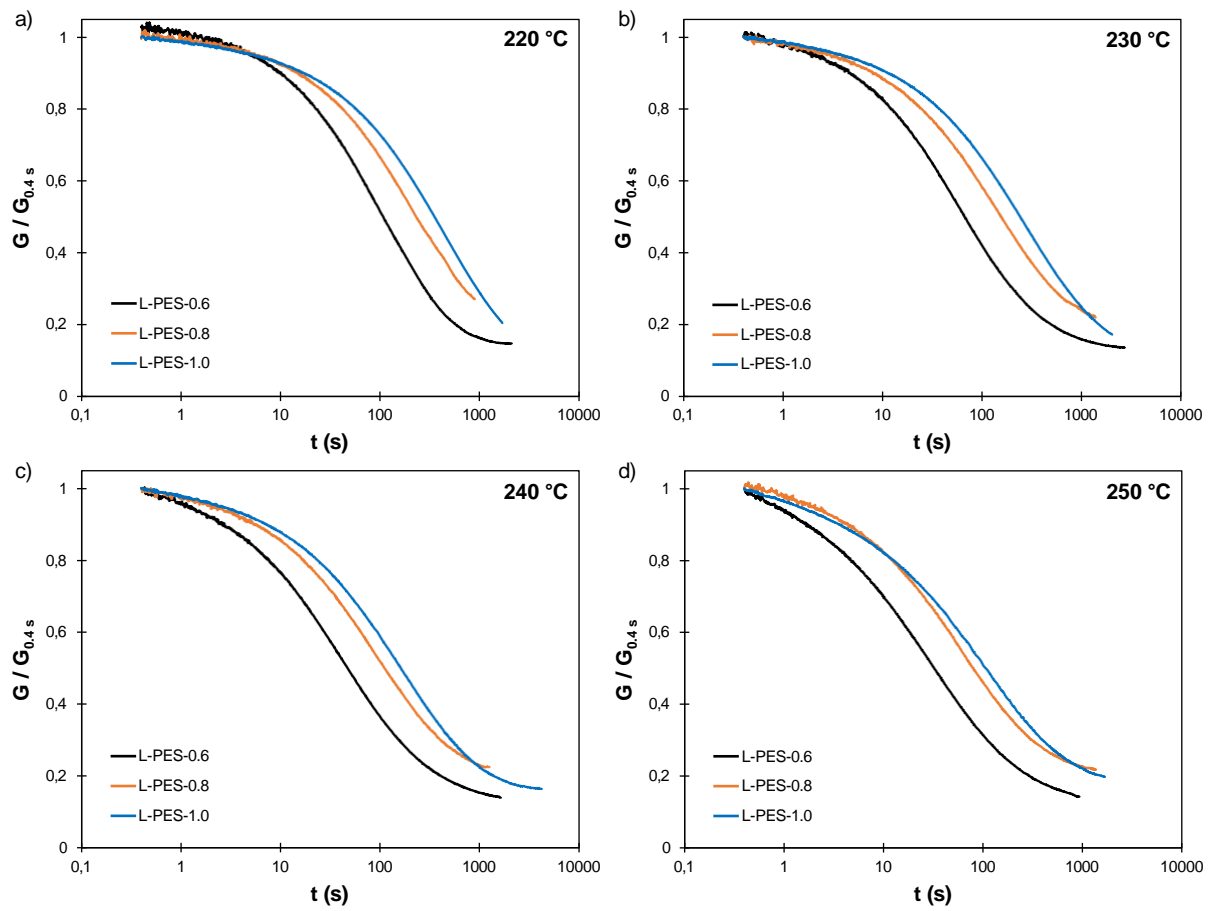
Figure S 18. Normalized stress relaxation curves of the different materials at (a) 220, (b) 230, (c) 240 and (d) 250 °C.
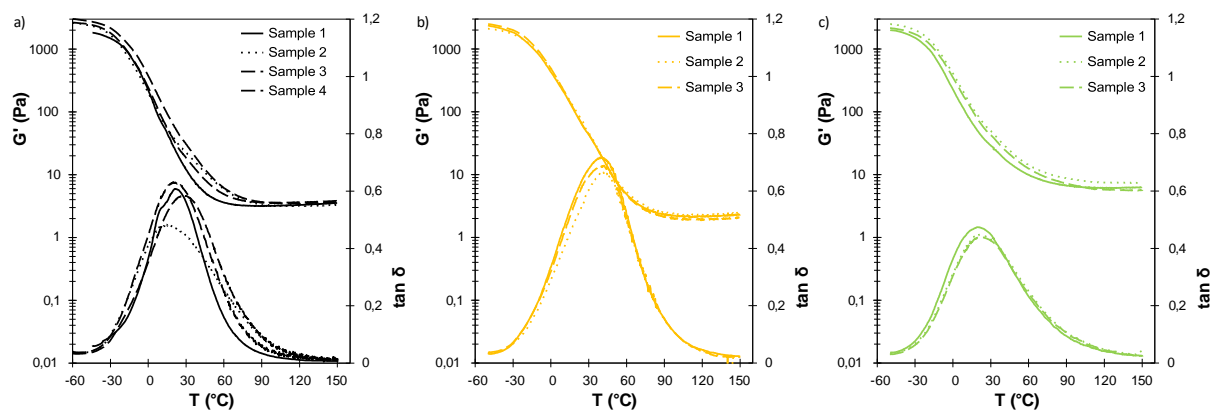
Figure S 19. Replicates of DMA of L-PES-0.8: (a) virgin material, (b) mechanically recycled and (c) chemically recycled.
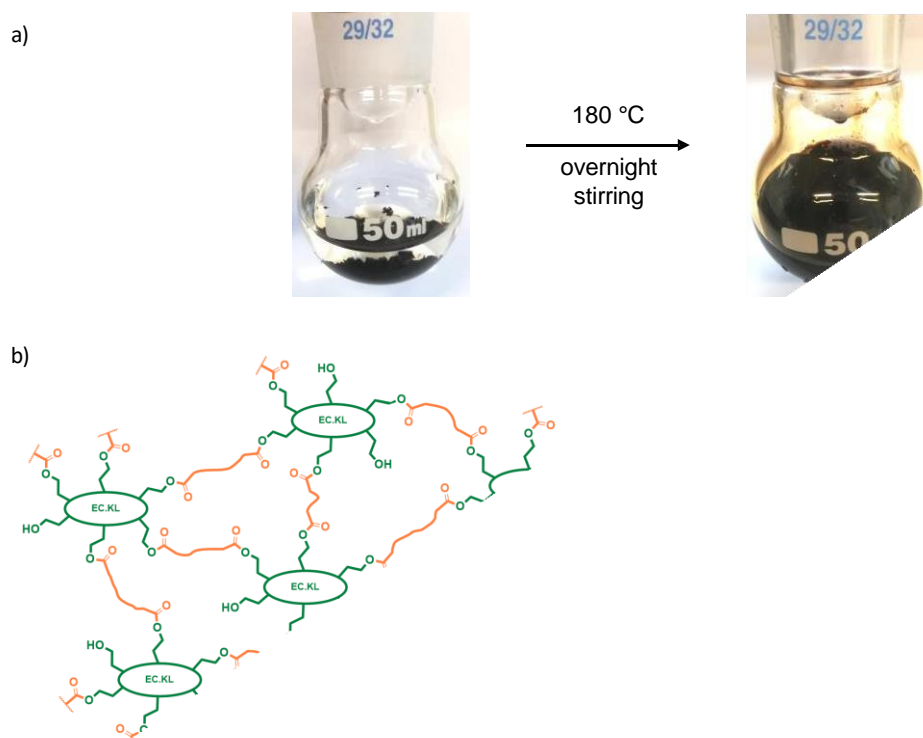

Figure S 20. Dissolution of L-PES network in ethylene glycol (EG): (a) pictures of the reaction mixture before and after overnight dissolution, (b) scheme of the network disruption by transesterification with EG.
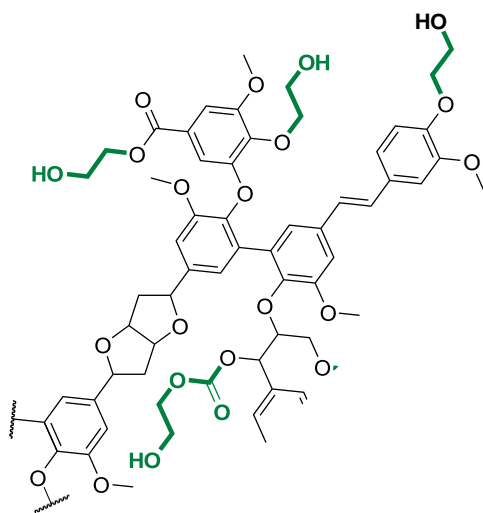
Figure S 21. Potential structure found in r.KL.EC-150, with PEG-COOH (in orange) esterified with EG (in maroon) bound to the lignin.

Table S 12. Results of dissolution of L-PES-0.8 in EG and recovery of r.KL.EC depending on the temperature

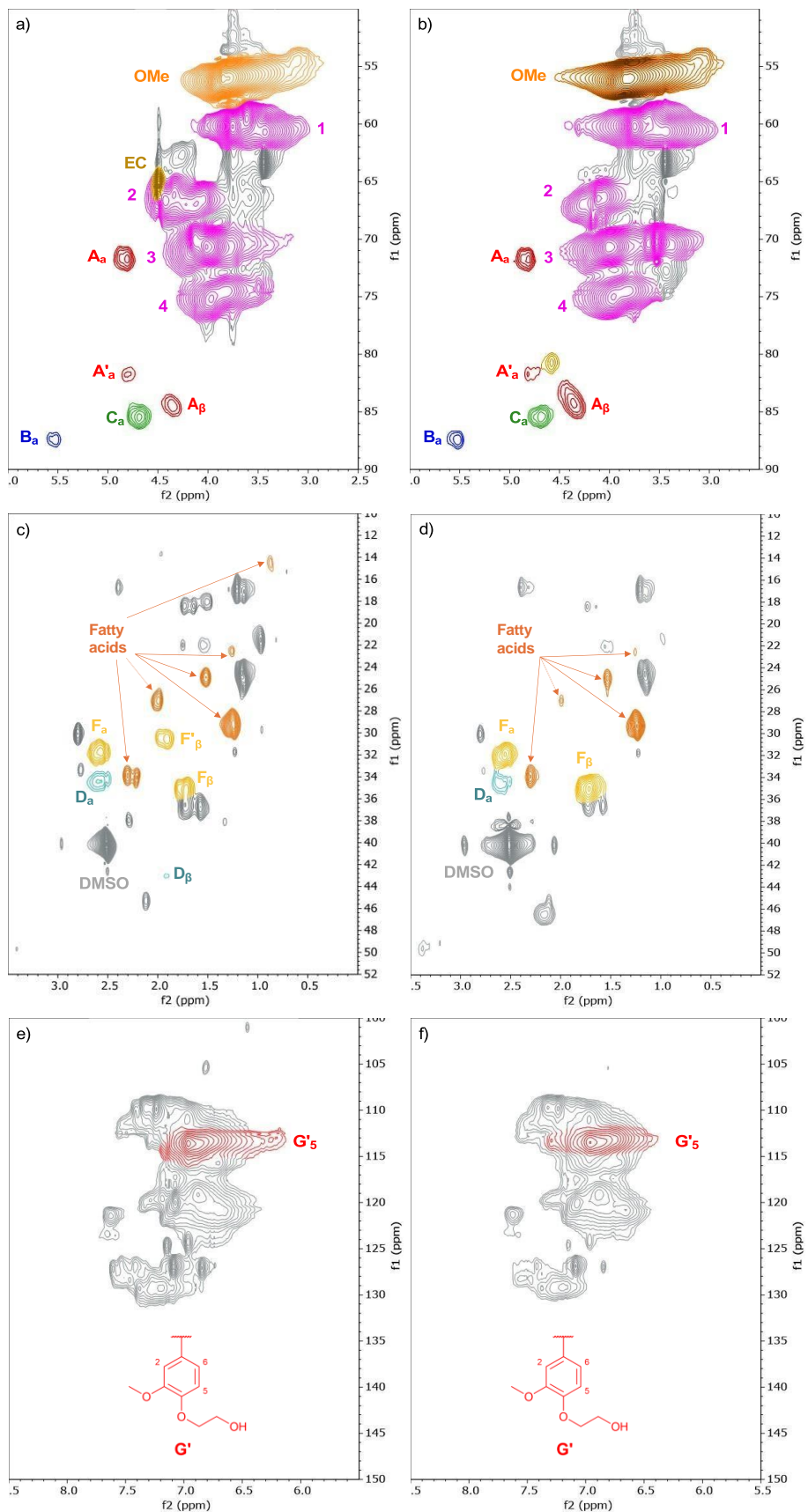| T (℃)	Soluble fraction (%)	r.KL.EC recovery (%)	
		based on soluble fraction	*based on total*
150	69.4	39.1	27.1
180	99.9	84.3	84.2

Figure S 22. (a,b) Aliphatic side chain, (c,d) alkyl and (e,f) aromatic regions of HSQC NMR spectra of KL.EC (a,c,e) and r.KL.EC-180 (b,d,f).
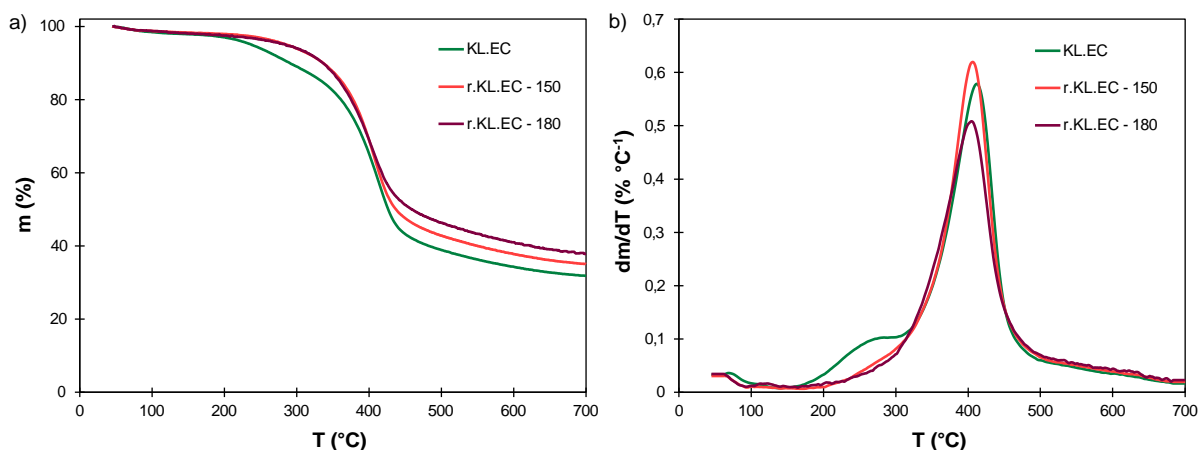
Figure S 23. TGA of neat and recycled KL.EC: (a) mass loss and (b) derivative weight loss (DTG curves).

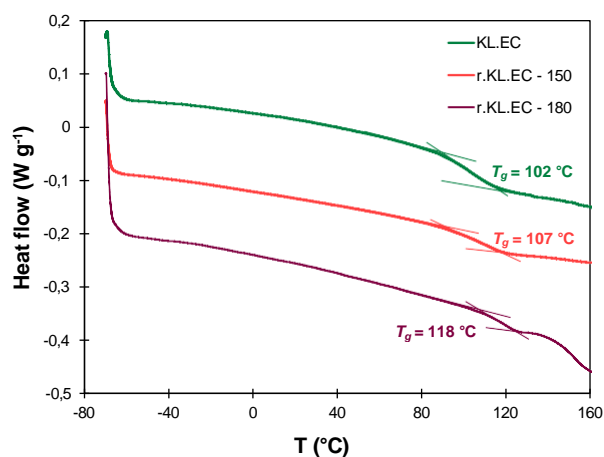*Figure S 24. DSC thermograms of neat and recycled KL.EC.*

References

1 A. DeVierno Kreuder, T. House-Knight, J. Whitford, E. Ponnusamy, P. Miller, N. Jesse, R. Rodenborn, S. Sayag, M. Gebel, I. Aped, I. Sharfstein, E. Manaster, I. Ergaz, A. Harris and L. Nelowet Grice, *ACS Sustainable Chem. Eng.*, 2017, **5**, 2927–2935.

2 Y. Xu, K. Odelius and M. Hakkarainen, *ACS Sustainable Chem. Eng.*, 2019, **7**, 13456–13463.

3 S. Zhang, T. Liu, C. Hao, L. Wang, J. Han, H. Liu and J. Zhang, *Green Chem.*, 2018, **20**, 2995–3000.

4 C. Hao, T. Liu, S. Zhang, L. Brown, R. Li, J. Xin, T. Zhong, L. Jiang and J. Zhang, *ChemSusChem*, 2019, **12**, 1049–1058.

5 L. Du, X. Jin, G. Qian, W. Yang, L. Su, Y. Ma, S. Ren and S. Li, *Industrial Crops and Products*, 2022, **187**, 115439.